diffusion-fundamentals

The Open-Access Journal for the Basic Principles of Diffusion Theory, Experiment and Application

Parameter dependence of ballistic velocity in deterministic diffusion in the form of devil's staircase

Syuji Miyazaki, Masaomi Yoshida and Hirokazu Fujisaka

Graduate School of Informatics, Kyoto University, Kyoto 606-8501, JAPAN, E-mail: syuji@acs.i.kyoto-u.ac.jp

Abstract

By using simple extended mapping models showing chaotic diffusion, non-perturbative non-Gaussian characteristics of diffusive motion are examined in the framework of the large deviation statistical theory. Furthermore, by rigorously solving the large deviation statistical quantities, it is found that the same type of anomalous, complex control parameter dependence as that for the diffusion coefficient reported by Klages and Dorfman is also observed in the large deviation statistical quantities such as the weighted average, the generalized diffusion coefficient and the generalized power spectrum densities.

1 Introduction

Diffusion is one of the most important and widely observed phenomena not only in statistical and chemical physics but also in other fields of science and engineering. For a statistically steady random variable u_t, the variable X_t generated by the dynamics

$$X_{t+1} = X_t + u_t, \quad (t = 0, 1, 2, 3, \cdots) \tag{1}$$

shows a diffusive motion. Namely, the variance of X_t, $\sigma_0^2(t) \equiv \langle (X_t - X_0 - \langle u \rangle t)^2 \rangle$, $\langle \cdots \rangle$ being the ensemble average of $\cdots$, obeys the law $\sigma_0^2(t) \approx 2Dt$ for large t. The diffusion coefficient D is a key quantity to characterize the statistics of the diffusive process.

The diffusion process is observed also in chaotic dynamics [1]. Namely, if the quantity u_t is generated by the chaotic dynamics and has the mixing property, i.e., the time correlation function of u_t decays in an appropriately fast way, the quantity X_t shows diffusive statistics. This phenomenon is called either *deterministic diffusion* or *chaotic diffusion* and is one of the eminent characteristics in nonlinear dynamics.

In order to study the diffusive statistics, the diffusion coefficient is quite important. This is because the diffusion coefficient is directly related to the asymptotic

Diffusion Fundamentals 3 (2005) 9.1 - 9.34

form of the maximum region of the probability density for the variable X_t as

$$P_t(X) \sim \exp\left[-S\left(\frac{X-X_0}{t}\right)t\right], \quad (2)$$

$$S(u) = \frac{1}{4D}\left(u-\langle u\rangle\right)^2 \quad (3)$$

for large t [2]. Because of the central limit theorem, this Gaussian form holds even if the variable u_t is very different from the Gaussian random variable. The diffusion coefficient D thus cannot describe the non-Gaussian statistics of X_t in an appropriate manner. The non-Gaussian characteristics, which are observed typically in the tail regions of $P_t(X)$, are analyzed in the framework of the large deviation statistical theory [2]. This analysis leads to the concept of the "fluctuation of diffusion coefficient"[2]. The generalized diffusion coefficient, which is explained in detail in Sec. II, can describe various statistics of X_t and u_t including non-ballistic and ballistic motions in a clear-cut way.

On the other hand, Klages and Dorfman recently reported a complex, anomalous control parameter dependence of diffusion coefficients, taking simple chaotic mapping dynamics showing diffusive motion (*fractal diffusion coefficient*) [3]. This complex behavior reflects the existence of infinitely many unstable limit cycles in the state space.

As explained above, there are two interesting problems in the statistical characterization of chaotic diffusion, large deviation characterization and the complex control parameter dependence of statistical quantities for diffusive motion. The fundamental purpose of the present paper is to examine chaotic diffusive motion from the viewpoint of large deviation statistics and the complex control dependence of statistical quantities. Particularly, we pay attention to how the complex control parameter dependence is observed in the large deviation statistical quantities.

The present paper is organized as follows. In Sec. II, we briefly review the formalism of the large deviation statistical analysis of diffusive motion to describe non-perturbative non-Gaussian characteristics of diffusive motion. Furthermore, the formulae to determine the statistical quantities of large deviation statistical quantities in chaotic dynamics are summarized. In Sec. III, taking a simple mapping model to generate chaotic diffusion, we show how the formulae to statistical quantities work. In Sec. IV, extending the chaotic mapping model given in Sec. II, we study how the control parameter affects the diffusion characteristics such as the conventional diffusion coefficient and the large deviation statistical quantities. It will be found that for the present models a complex control parameter dependence of diffusion coefficients is observed, and we will find that such an anomalous control parameter dependence is observed also in the large deviation statistical quantities. By listing the results obtained in the present paper, we give a conclusion in Sec. V.

Diffusion Fundamentals 3 (2005) 9.1 - 9.34

2 Description of non-Gaussian fluctuation

2.1 Framework of large-deviation statistics

Let us briefly describe large deviation statistics following the series of studies by Fujisaka and his coworkers [4, 5, 6, 7, 8, 9]. Consider a stationary time series u. The average over time interval T is given by this formula,

$$\bar{u}_T(t) = \frac{1}{T}\int_t^{t+T} u_s ds \tag{4}$$

which distributes when T is finite. When T is much larger than the correlation time of u, the distribution $P_T(u)$ of coarse-grained u is assumed to be an exponential form $P_T(u) \propto \mathrm{e}^{-S(u)T}$. Here we can introduce the fluctuation spectrum $S(u)$ as

$$S(u) = -\lim_{T\to\infty}\frac{1}{T}\log P_T(u) \quad (S(u) \geq 0) \tag{5}$$

When T is comparable to the correlation time, correlation cannot be ignored, so non-exponential or non-extensive statistics will be a problem, but here we do not discuss this point further. Let q be a real parameter. We introduce the generating function Z_q of T by this definition.

$$Z_q(T) \equiv \left\langle e^{qT\bar{u}_T}\right\rangle = \int_{-\infty}^{\infty} P_T(u)e^{qTu}du \tag{6}$$

We can also here assume the exponential distribution and introduce characteristic function $\phi(q)$ as

$$\phi(q) = \lim_{T\to\infty}\frac{1}{T}\log Z_q(T) \tag{7}$$

The Legendre transform holds between fluctuation spectrum $S(u)$ and characteristic function $\phi(q)$, which is obtained from saddle-point calculations.

$$\frac{dS(u)}{du} = q, \quad \phi(q) = -S(u(q)) + qu(q) \tag{8}$$

In this transform a derivative $d\phi/dq$ appears, and it is a weighted average of $\overline{u}_T$,

$$u(q) = \phi'(q) = \lim_{T\to\infty}\frac{\left\langle \bar{u}_T e^{qT\bar{u}_T}\right\rangle}{Z_q(T)} \equiv \lim_{T\to\infty}\langle \bar{u}_T; q\rangle_T \tag{9}$$

so we find that q is a kind of weight index. We can also introduce susceptibility $\chi(q) = \dfrac{du(q)}{dq}$ as a weighted variance. These statistical structure functions $S(u), \phi(q), u(q), \chi(q)$ constitute the framework of statistical thermodynamics of temporal fluctuation, which characterize static properties of chaotic dynamics. In order

Diffusion Fundamentals 3 (2005) 9.1 - 9.34

to consider dynamic properties, we can introduce this generalized spectrum density as a weighted average of normal spectrum density.

$$I_q(\omega) = \lim_{T\to\infty} \frac{1}{T} \frac{\left\langle \left| \int_0^T [u\{t+s\} - u(q)] \mathrm{e}^{-i\omega s} ds \right|^2 \mathrm{e}^{qT\overline{u}_T} \right\rangle}{Z_q(T)}.$$

2.2 Generalization of diffusion coefficients

Fujisaka and Inoue applied this large-deviation statistical analysis to diffusion processes [2]. In the following, we restrict $u(q)$ to weighted averages of velocity obtained from a diffusion process. Equation (9) leads to

$$u'(q) = \lim_{t\to\infty} \frac{1}{t} \left\langle (x_t - x_0 - u(q)t)^2; q \right\rangle_t, \tag{10}$$

where x_t denotes position at time t. In Eqs. (9) and (10), $u(0)$ $(= \phi'(0))$ and $u'(0)$ $(= \phi''(0))$ are respectively identical to the drift velocity v_d and $2D$, where D is the diffusion coefficient. Therefore, $u(q)$ may be regarded as the generalized drift velocity (order-q drift velocity). Furthermore, the generalized variance (order-q variance) defined by

$$\sigma_q^2(t) \equiv \left\langle (x_t - x_0 - u(q)t)^2; q \right\rangle_t = t^2 \left\langle (\bar{u}_t - u(q)t)^2; q \right\rangle_t, \tag{11}$$

asymptotically takes the form

$$\sigma_q^2(t) = 2D_q t, \tag{12}$$

for large t, where

$$D_q \equiv \lim_{t\to\infty} \frac{\sigma_q^2(t)}{2t} = \frac{u'(q)}{2} = \frac{\chi(q)}{2} = \frac{1}{2S''(u(q))}. \tag{13}$$

By introducing the generalized (order-q) time correlation function by

$$C_q(s) = \lim_{t\to\infty} \frac{\langle (u_s - u(q))(u_0 - u(q)) e^{qt\bar{u}_t} \rangle}{Z_q(t)}, \tag{14}$$

the generalized (order-q) diffusion coefficient is expressed as

$$D_q = \int_0^\infty C_q(s) ds, \tag{15}$$

where $D_{q=0}$ is identical to the ordinary diffusion coefficient.

Applying the cumulant expansion to $Z_q(t)$, $\phi(q)$ is expanded as

$$\phi(q) = \phi'(0)q + \frac{1}{2}\phi''(0)q^2 \tag{16}$$

Diffusion Fundamentals 3 (2005) 9.1 - 9.34

provided that $|q|$ is much less than the convergence radius q_0 of the expansion. This immediately leads to

$$u(q) = \phi'(0) + \phi''(0)q, \tag{17}$$

$$S(u) = \frac{(u - \phi'(0))^2}{2\phi''(0)} \quad (\geq 0). \tag{18}$$

The Gaussian approximation holds for u satisfying $|u - \phi'(0)|/\phi'(0) \ll q_0$. If u_t is Gaussian, the $q_0 = +\infty$ and (18) holds for any u. Therefore, the non-Gaussian property causes the q-dependence of D_q, which is the origin of the existence of an infinite number of statistical characteristics of diffusive motion.

2.3 Relationship between generalized Frobenius-Perron operators and statistical structure functions for one-dimensional mapping systems

Let us consider the case of a one-dimensional map. Let $u[x_n]$ be a unique function of x, which is governed by the map $x_{n+1} = f(x_n)$. The question is how to obtain statistical structure functions and generalized spectral densities of u. The answer is to solve eigenvalue problems of a generalized Frobenius-Perron operator. As we mentioned before, the characteristic function $\phi(q)$ is given by the asymptotic form of the generating function $Z_q(n)$ in the limit of $n \to \infty$ corresponding to the temporal coarse-grained quantity $\overline{u}_n = \dfrac{1}{n}\displaystyle\sum_{j=0}^{n-1} u[x_{j+m}]$, where we assume an exponential fast decay of time correlations of u. A generating function can be expressed in terms of invariant density,

$$\begin{aligned} Z_q(n) &\equiv \left\langle e^{q\,n\bar{u}_n} \right\rangle \\ &= \int \rho^*(x) \exp\left[q \sum_{j=0}^{n-1} u\left[f^j(x)\right] \right] dx \\ &= \int \mathcal{H}_q^n \rho^*(x) dx, \end{aligned} \tag{19}$$

where the generalized Frobenius-Perron operator $\mathcal{H}_q$ is defined and related to the original one as

$$\mathcal{H}_q G(x) = \mathcal{H}\left[e^{q\,u[x]} G(x) \right] = \sum_j \frac{e^{q\,u[y_j]} G(y_j)}{|f'(y_j)|} \tag{20}$$

for an arbitrary function $G(x)$ ($\mathcal{H}_0 = \mathcal{H}$), where the sum is taken over all solutions $y_j(x)$ satisfying $f(y_j) = x$. To obtain the above equation, the following relation is repeatedly used:

$$\mathcal{H}\left\{ G(x) \exp\left[q \sum_{j=0}^{m} u[f^j(x)] \right] \right\} = (\mathcal{H}_q G(x)) \exp\left[q \sum_{j=0}^{m-1} u[f^j(x)] \right].$$

Diffusion Fundamentals 3 (2005) 9.1 - 9.34

Let $\nu_q^{(0)}$ be the maximum eigenvalue of H_q. The characteristic function is given by its logarithm as

$$\phi(q) = \log \nu_q^{(0)}, \quad \left(\nu_0^{(0)} = 1\right). \tag{21}$$

The weighted average $u(q)$ and the susceptibility $\chi(q)$ is given by the first and the second derivative of $\phi(q)$.

The generalized power spectrum is as

$$I_q(\omega) = \int v^{(0)}(x)[u[x] - u(q)][J_q(\omega) + J_q(-\omega) - 1][u[x] - u(q)]h^{(0)}(x)dx, \tag{22}$$

where $J_q(\omega) = 1/\left[1 - (\mathrm{e}^{i\omega}/\nu_q^{(0)})\mathcal{H}_q\right]$, $v^{(0)}(x)$ and $h^{(0)}(x)$ are respectively left and right eigenfunctions corresponding to the maximum eigenvalue $\nu_q^{(0)}$ of $\mathcal{H}_q$.

3 Simple example of deterministic diffusion

It is usually difficult to obtain statistical structure functions by means of analysis. However, in simple systems such as piecewise linear maps, it is sometimes possible to analytically calculate such functions depending on the parameters involved in the systems. This chapter will introduce piecewise linear maps which present with chaotic diffusion and will set the parameters of these systems at the simplest value which allows Markov partition, with the goal of analytically deducing statistical structure functions such as a generalized diffusion coefficient D_q and a generalized power spectrum $I_q(\omega)$.

3.1 Piecewise linear maps and chaotic diffusion

Let us take an example of the following map:

$$\begin{aligned} & x_{n+1} = f(x_n) = \\ & \begin{cases} a(x_n - N) + N, & (N < x_n \le N + \frac{1}{2}), \\ a(x_n - N - 1) + N + 1, & (N + \frac{1}{2} < x_n \le N + 1), \end{cases} \\ \text{for} \quad & {}^{\forall}N \in \mathbb{N}. \end{aligned} \tag{23}$$

This is a piecewise-linear map depicted by drawing two lines (with a gradient of a) from the lower left vertex to the upper right vertex within a 1×1 square and arranging them in a stepwise manner as shown in Fig. 1.

If parameter a is set as $a > 2$ and an appropriate initial point except for unstable periodic points is given to it, the time series $\{x_n\}$ will show chaotic motion, resembling random walks. If mapping is repeated, while placing several initial points close to each other, individual points will gradually part from each other, resembling diffusion (Fig. 2)

Diffusion Fundamentals 3 (2005) 9.1 - 9.34

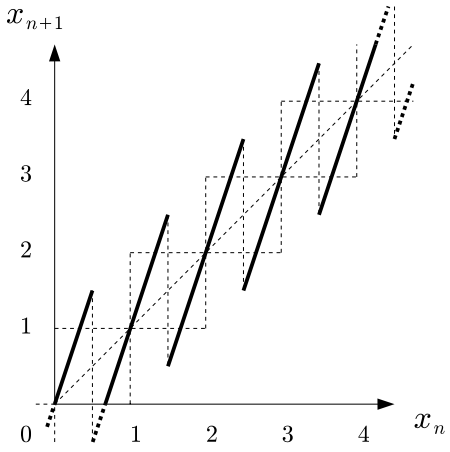

Figure 1: Piecewise-linear map

Unlike ordinary diffusion which is induced by random factors such as thermal motion of molecules, etc., this map can show diffusive motion which is determined only by the mixing property of the chaotic map and not by any stochastic elements, if the initial point is fixed. Such diffusion is called chaotic diffusion; it is sometimes called " deterministic diffusion " on the grounds that subsequent motions are determined by the initial point in a deterministic manner [10, 11, 12].

Now, let us consider how we can obtain the generalized diffusion coefficient D_q and the generalized power spectrum I_q in this mapping system. In a simple piecewise linear mapping system like this one, it is sometimes possible to obtain statistical structure functions analytically by setting the parameters of this system at levels which allow Markov partition. At one of the simplest values of the parameter allowing Markov partition, we will describe the method for statistically deducing D_q and I_q, using generalized Frobenius-Perron operator H_q.

3.2 Markov partition of piecewise linear maps and their expression using the matrix of generalized Frobenius-Perron operator

Regarding Eq. (23) shown in the preceding section, let us consider replacing the location x_n of particles at time n with $x_n = X_n + x'_n$. Here X_n and x'_n are respectively the integer and fractional part of x_n. Now, Eq. (23) can be rewritten as

Diffusion Fundamentals 3 (2005) 9.1 - 9.34

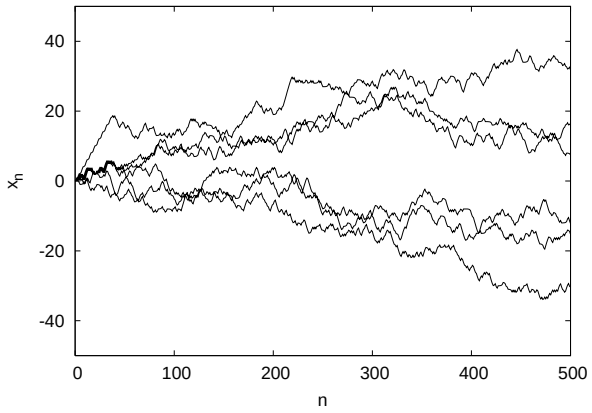

Figure 2: Chaotic diffusion

follows.

$$\begin{cases} X_{n+1} &= X_n + \Delta(x'_n), \\ x'_{n+1} &= g(x'_n), \\ \Delta(x'_n) &= \lfloor f(x'_n) \rfloor, \\ g(x'_n) &= f(x'_n) - \lfloor f(x'_n) \rfloor, \end{cases} \qquad (X_n \in \mathbb{N},\ 0 < x'_n \leq 1) \tag{24}$$

Equation (24) can be graphically represented as shown in Figs. 3-4. The map g defined by Eq. (24) is a chaotic map. For almost all the initial points, the trajectories become chaotic, as shown in Fig. 5.

In Fig. 3, the motion of X_n can be viewed as random walk on the one-dimensional lattice, with the lattice point $\Delta(x'_n)$ of each cell serving as a jump. In Eq. (24), the time series $\{X_n\}$ is dependent only on $\{x'_n\}$. In other words, $\{X_n\}$ is generated from the map g. As described in the previous section, the diffusion coefficient D_q of X_n's motion can be obtained if the generalized Frobenius-Perron operator H_q for g is given.

If $a = 1 + \sqrt{3}$, the map g assumes the form shown in Fig. 6. In this case, the map can be subjected to Markov partition. If all points within $p_{1,4}$ in each of the Markov cells $p_{1,2,3,4}$ shown in Fig. 6 are one-time maps, they can be mapped into one of p_1, p_2, p_3 and p_4 (i.e., can be mapped to the cell $p_{1+2+3+4}$). On the other hand, all points in $p_{2,3}$ can be mapped only to the cell $p_{1,4}$, respectively. Therefore, if this map is subjected to time evolution, with the initial distribution being uniform, the probability distribution at all times is constant within each Markov cell. This means that in maps which can be subjected to Markov partition, the generalized Frobenius-Perron operator of the map can be expressed in the form of a matrix. The generalized Frobenius-Perron operator, $H_q(a)$, can usually be expressed by the

Diffusion Fundamentals 3 (2005) 9.1 - 9.34

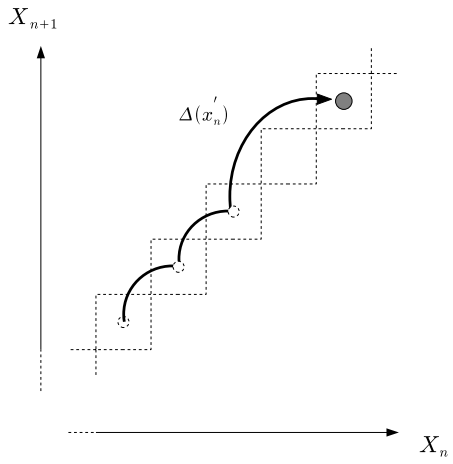

Figure 3: Dynamics of X_n

following matrix if $a = 1 + \sqrt{3}$.

$$
\begin{aligned}
H_q\left(1+\sqrt{3}\right) &= \frac{1}{1+\sqrt{3}} \begin{pmatrix} 1 & 1 & 0 & 1 \\ 1 & 0 & 0 & 1 \\ 1 & 0 & 0 & 1 \\ 1 & 0 & 1 & 1 \end{pmatrix} \\
&\quad \times \begin{pmatrix} e^{q\cdot 0} & 0 & 0 & 0 \\ 0 & e^{q\cdot 1} & 0 & 0 \\ 0 & 0 & e^{q\cdot(-1)} & 0 \\ 0 & 0 & 0 & e^{q\cdot 0} \end{pmatrix} \qquad (25) \\
&= \frac{1}{1+\sqrt{3}} \begin{pmatrix} 1 & e^{q} & 0 & 1 \\ 1 & 0 & 0 & 1 \\ 1 & 0 & 0 & 1 \\ 1 & 0 & e^{-q} & 1 \end{pmatrix} \qquad (26)
\end{aligned}
$$

Of the matrices contained in Eq. (25), the left matrix indicates the connections of each Markov cell. If cell p_i is mapped into cell p_j, the row j line i component of this matrix is defined as 1. If cell p_i is not mapped into cell p_j, this component is defined as 0. In the right matrix, the i-th diagonal component is $\exp(q \cdot \Delta_i)$ (Δ_i indicates the value of Δ corresponding to cell p_i) and is equivalent to $\mathrm{e}^{q\,u[x]}$ of Eq. (20).

Klages and Dorfman imposed periodic boundary conditions on their Markov process. In other words, they truncated infinite dimensional transition matrices to obtain conventional diffusion coefficients [3]. In contrast, we introduced the integer and fractional parts of dynamics in Eq. (24), so that we have only to solve eigenvalue

Diffusion Fundamentals 3 (2005) 9.1 - 9.34

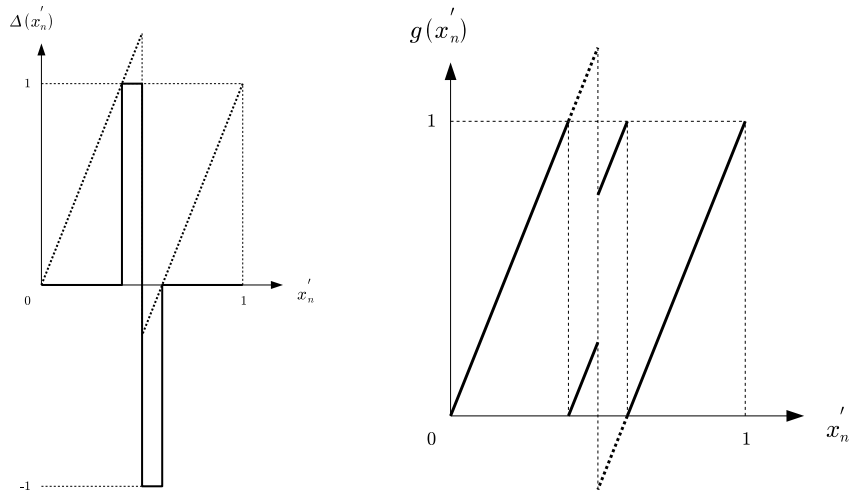

Figure 4: $\Delta(x_n')$ and $g(x_n')$

problems of *finite* dimensional generalized Frobenius-Perron matrices H_q. This is based on the fact that (generalized) diffusion coefficients are determined by the correlation functions of the velocity, namely, the fractional part of the dynamics only. Thus, we can obtain generalized diffusion coefficients including conventional ones more precisely without using matrix truncation.

3.3 Deduction of statistical structure functions and $D_q(a)$ and $I_q(a,\omega)$ when $a = 1+\sqrt{3}$

The maximum eigenvalue $\nu_q^{(0)}(a)$ of matrix $H_q(a)$ when $a = 1+\sqrt{3}$ can be calculated as follows:

$$\nu_q^{(0)}\left(1+\sqrt{3}\right) = \frac{e^q + \sqrt{e^q(e^{2q}+e^q+1)}}{\left(1+\sqrt{3}\right)e^q}. \tag{27}$$

From this value, we can deduce the statistical structure functions for the time series of the velocity of the chaotic diffusion $\{\Delta(x_n')\}$ as follows.

$$\begin{aligned}\phi(q)\Big|_{a=1+\sqrt{3}} &= \log\nu_q^{(0)}\left(1+\sqrt{3}\right) \\ &= \log\frac{A_1+A_2}{\left(1+\sqrt{3}\right)A_1},\end{aligned} \tag{28}$$

$$u(q)\Big|_{a=1+\sqrt{3}} = \phi'(q)\Big|_{a=1+\sqrt{3}} = \frac{A_1\left(A_1^2-1\right)}{2A_2A_3}, \tag{29}$$

Diffusion Fundamentals 3 (2005) 9.1 - 9.34

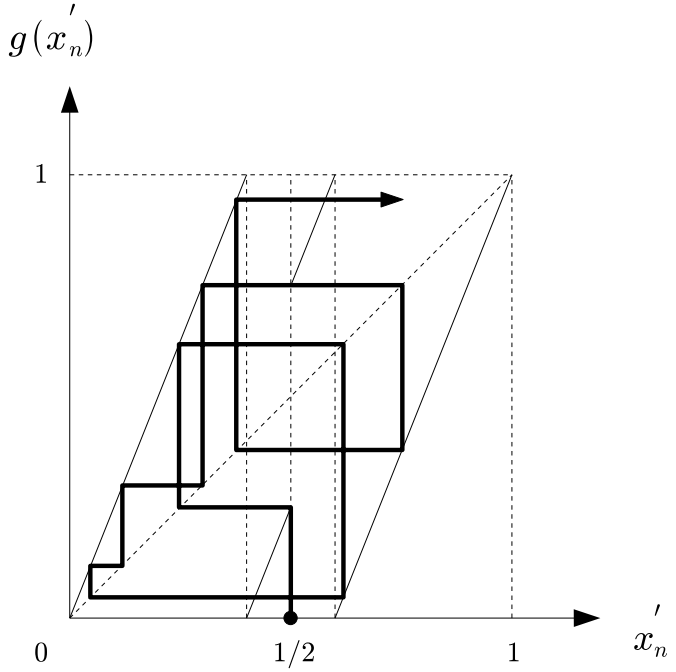

Figure 5: Trajectory starting from the initial point $x_0 = 1/2$

$$D_q\left(1+\sqrt{3}\right) = \frac{A_1^3}{8A_2^3A_3^2} \times (A_1^4 + 2A_1^3 + 2A_1^2A_2 + 6A_1^2 + 8A_1A_2 + 2A_1 + 2A_2 + 1), \tag{30}$$

$$I_q\left(1+\sqrt{3},\ \omega\right) = \frac{B_1\cos\omega + B_2}{B_3\cos\omega + B_4} \times \frac{(A_1 - A_2)(A_1^3 - A_2)}{2A_1(A_1^2 - A_1^2A_2 + A_1 + 1)(A_1^2 + 1)}, \tag{31}$$

Diffusion Fundamentals 3 (2005) 9.1 - 9.34

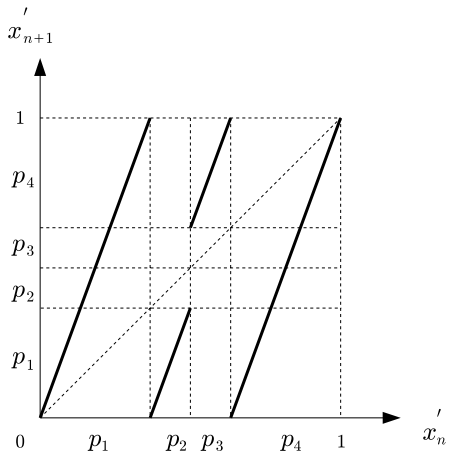

Figure 6: Map g for $a = 1 + \sqrt{3}$

where

$$
\begin{aligned}
A_1 &= e^q, \\
A_2 &= \sqrt{e^q(e^{2q} + e^q + 1)}, \\
A_3 &= e^q + \sqrt{e^q(e^{2q} + e^q + 1)}, \\
B_1 &= 4A_1^4 + 8A_1^3 + 8A_1^2A_2 + 4A_1^2, \\
B_2 &= 3A_1^5 + A_1^4A_2 + 8A_1^4 + 4A_1^3A_2 + 10A_1^3 \\
&\quad +6A_1^2A_2 + 8A_1^2 + 4A_1A_2 + 3A_1 + A_2, \\
B_3 &= A_1^4 + 2A_1^3 + 2A_1^2A_2 + 2A_1^2 + 2A_1 + 2A_2 + 1, \\
B_4 &= A_1^4 + 4A_1^3 + 2A_1^2A_2 + 6A_1^2 + 4A_1A_2 + 4A_1 \\
&\quad +2A_2 + 1.
\end{aligned}
$$

These equations are graphically represented in Fig. 7 through 10.

The $u(q)$ shown in Fig. 8 is a weighted average of the time series of the velocity of the chaotic diffusion $\{\Delta(x'_n)\}$. According to the framework of the theory of large deviation statistics, u at $q = 0$, i.e. $u(q = 0)$, should be equal to 0, identical to the ordinary average $\{\Delta(x'_n)\}$ due to the symmetry of the map g. In fact, $u(0)$ is equal to 0 in the graph. In the same way, $D_0(1 + \sqrt{3})$ at a q value of 0 is identical to the diffusion coefficient D (Fig. 9), and the $I_0(1 + \sqrt{3}, \omega)$ in Fig. 10 is equal to the conventional power spectrum obtained by the ordinary method, without involving weighting. If q is increased from 0 to ∞, the weighted average $u(q)$ increases, eventually approaching 1/2. That is, of the various processes involved in chaotic diffusion, the q corresponding to the process with largest fluctuation is equal to ∞, and the average velocity at that time is 1/2. In the same way, the generalized

Diffusion Fundamentals 3 (2005) 9.1 - 9.34

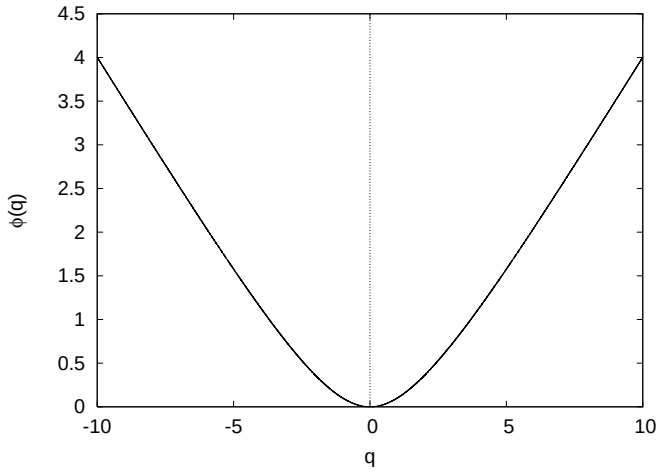

Figure 7: $\phi(q)$ $\left(a = 1 + \sqrt{3}\right)$

diffusion coefficient D_q also approaches the diffusion coefficient $D_\infty(1 + \sqrt{3}) = 0$, which corresponds to the process with largest fluctuation, as q increases to ∞. The generalized power spectrum $I_q(1 + \sqrt{3}, \omega)$ approaches the delta function $I_\infty(1 + \sqrt{3}, \omega) = \delta(\omega - \pi)$ as q increases to ∞. If we consider that the average of $\Delta(x'_n)$ is $1/2$, the diffusion coefficient is 0 and the power spectrum serves as a delta function, we may say that the orbit with the greatest fluctuation when $a = 1 + \sqrt{3}$, is the drift orbit (Fig. 11) occurring from the period two orbits of x'_n shown in Fig. 12.

4 Numerical calculation of generalized diffusion coefficient $D_q(a)$ and generalized power spectrum $I_q(a, \omega)$ and its results

It is known that in the chaotic diffusion system represented by Eq. (23) there is a complex dependence of diffusion coefficient $D(a)$ on parameter a. Our numerical calculation revealed that the generalized diffusion coefficient $D_q(a)$ and the generalized power spectrum $I_q(a, \omega)$ are also dependent on the parameter in a complex manner. It was additionally found that, among the various possible orbits for this system, the drift orbit shows a relationship between parameter a and average velocity that can be graphically represented in a form resembling the devil's staircase. This chapter will present these findings, using graphic representations.

Diffusion Fundamentals 3 (2005) 9.1 - 9.34

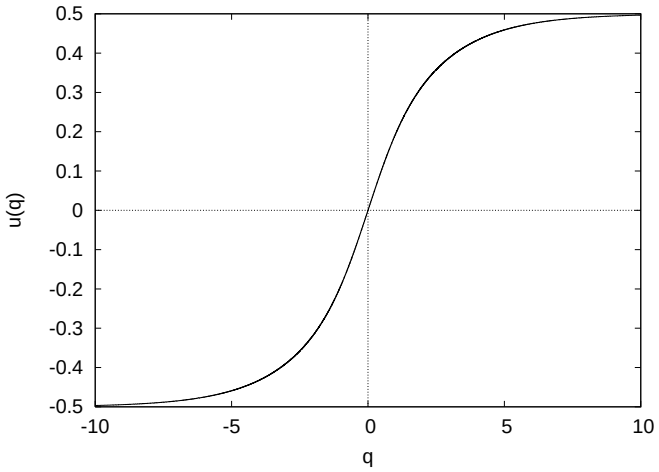

Figure 8: $u(q)$ $\left(a = 1 + \sqrt{3}\right)$

4.1 Numerical calculation of generalized diffusion coefficient D_q and its results

Klages and Dorfman discovered that a complex correlation is present between parameter a and diffusion coefficient $D(a)$ in the chaotic diffusion system defined by Eq. (23) [3]. Figure 13 graphically represents this relationship. They called the diffusion coefficient expressed by this curve a "fractal diffusion coefficient"on the grounds that more minute structures continue to appear within the irregular curve when a part of the curve is magnified with progressively higher powers [3, 13, 14, 15]. This curve represents an ordinary diffusion coefficient for this system. What curve will be depicted by the generalized diffusion coefficient, i.e., the diffusion coefficient expanded within the framework of the theory of large deviation statistics? To obtain this curve, we should first obtain values of a (for which Markov partition is possible) in a number large enough to fill the a-axis adequately. (See Appendix A for detail.) For each value of a thus obtained, we then calculate the maximum eigenvalue $\nu_q^{(0)}(a)$ of the generalized Frobenius-Perron operator $H_q(a)$ for the map g discussed in the preceding chapter. Then, the equation $D_q(a) = 1/2(\partial^2/\partial q^2) \log \nu_q^{(0)}(a)$ is used. In this way, the curve shown in Fig. 14 can be obtained. In Fig. 14, the curve for $q = 0$ is identical to the conventional diffusion coefficient $D(a)$ shown in Fig. 13. As q is gradually increased from 0, the curve descends, eventually converging at 0 when q approaches ∞. During this process, it appears that the peaks of the curve are gradually smoothed, resulting in a gradual increase in the percentage of the relatively linear parts in the entire curve. On the basis of this finding, we estimate that if the fractal dimension $d_f(q)$ for the curve $D_q(a)$ is measured, it will gradually

Diffusion Fundamentals 3 (2005) 9.1 - 9.34

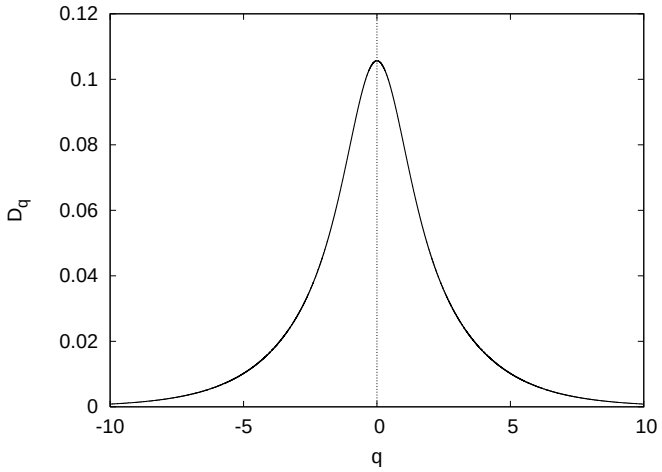

Figure 9: $D_q\left(1+\sqrt{3}\right)$

decrease from its value at $D_0(a)$, eventually approaching 1. Figure 15 shows the results of measuring the fractal dimension $d_f(q)$ of curve $D_q(a)$ at varying values of q, using the divider method.

Now we discuss the results of $d_f(q)$ measurement. Regarding the fractal dimension of $D_0(a)$, we obtained $d_f(0) \simeq 1.046$. This indicates that $d_f(q)$ shows monotone decrease until $q = 0.2$. If q is larger than 0.2, $d_f(q)$ depicts an upward convex curve. Maximum $d_f(q_{max}) \simeq 1.05$ was recorded when q_{max} was 0.6-0.7. In Fig. 14, the curve for $q = 0.7$ is shown in a solid line. The curve shown with this solid line can be viewed as having the highest fractal dimension among $D_q(a)$. As illustrated above, not only the diffusion coefficient $D(a)$ but also the generalized diffusion coefficient $D_q(a)$ assumed a complex form in the chaotic diffusion system defined by Eq. (23).

4.2 Numerical calculation of generalized diffusion coefficient $I_q(a,\omega)$ and its results

As described in Section 3.3, the generalized power spectrum $I_q(a,\omega)$ for a allowing Markov partition can be obtained by calculating $H_q(a)$ and its maximum eigenvalue $\nu_q^{(0)}(a)$ and the corresponding right and left eigenvectors and by applying these values to Eq. (22). Because $I_q(a,\omega)$ involves three variables (q,a,ω), the results of calculation need to be expressed on the $a-\omega$ plane for full characterization of $I_q(a,\omega)$. Figures 16 through 20 show the results of numerical calculation at $q = 0$, 1, 2, 5 and 10 in images. In these images, the horizontal direction indicates a and the vertical direction corresponds to ω. It presents the values of $I_q(a,\omega)$ at a given

Diffusion Fundamentals 3 (2005) 9.1 - 9.34

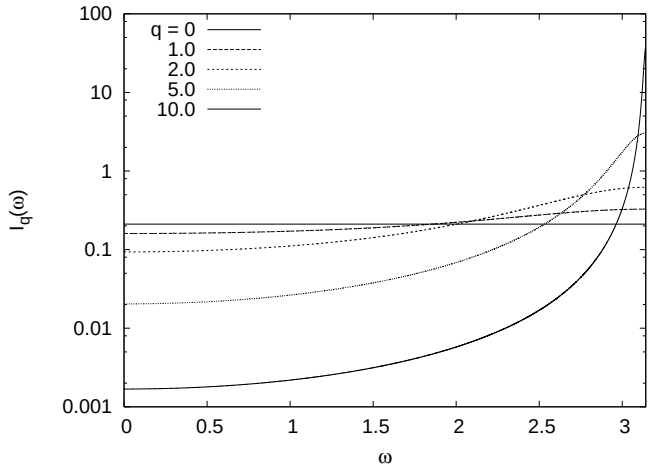

Figure 10: $I_q\left(1+\sqrt{3},\omega\right)$

point on the plane in a gray scale. (the number of points is equal to 600 in the a-direction, 314 in the ω-direction.)

Cross-sections of these 5 planes, cut horizontally along $\omega = 0, \pi/2, \pi$ are shown below. Each of Fig. 21 through 23 contains two graphs. The upper graph uses an ordinary scale, while the lower graph uses a logarithmic vertical scale.

Diffusion Fundamentals 3 (2005) 9.1 - 9.34

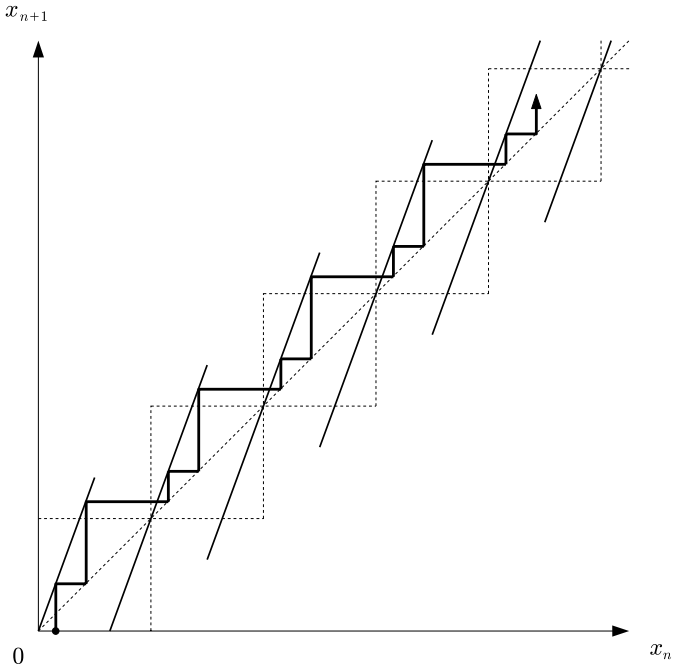

Figure 11: Period-two drift motion

Diffusion Fundamentals 3 (2005) 9.1 - 9.34

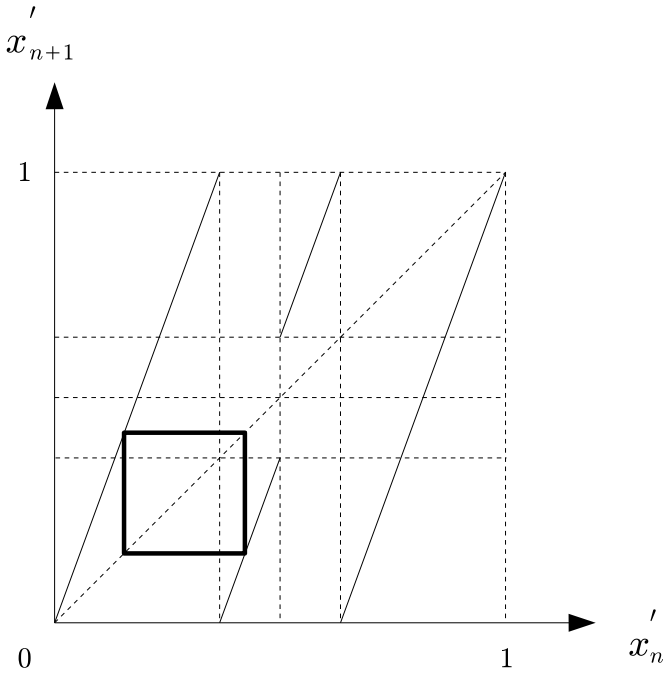

Figure 12: Period-two trajectory in the map g

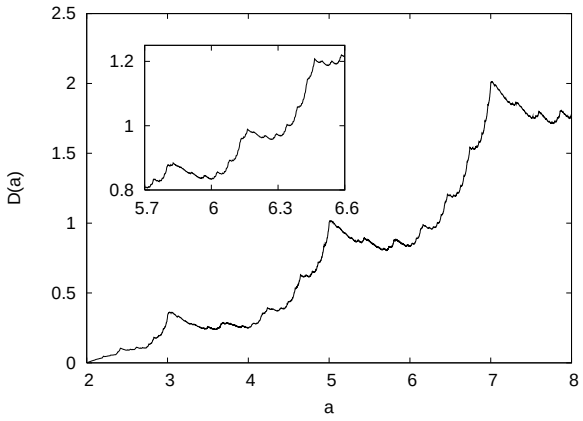

Figure 13: Complex parameter dependence of the diffusion coefficient $D(a)$

Diffusion Fundamentals 3 (2005) 9.1 - 9.34

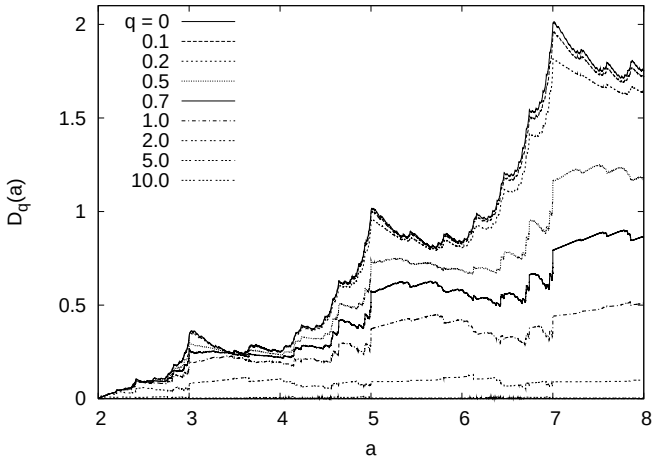

Figure 14: Generalized diffusion coefficient $D_q(a)$

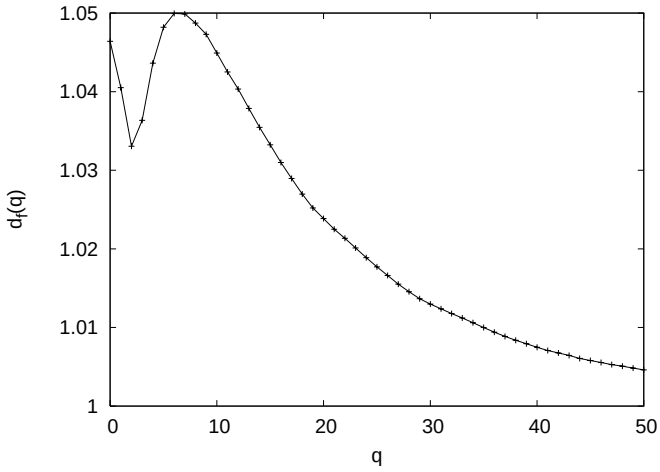

Figure 15: Fractal dimension $d_f(q)$ of $D_q(a)$

Diffusion Fundamentals 3 (2005) 9.1 - 9.34

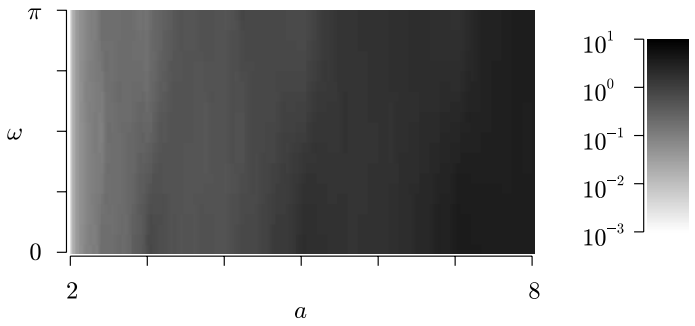

Figure 16: $I_{q=0}(a,\omega)$

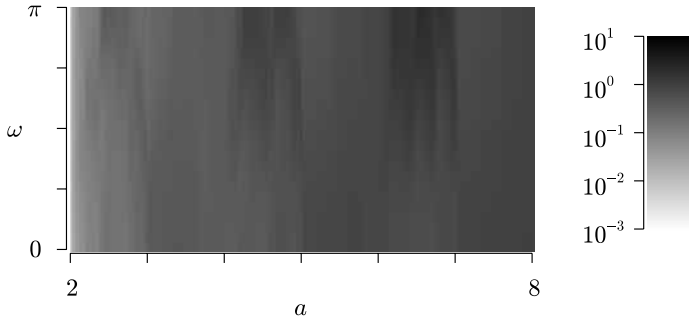

Figure 17: $I_{q=1}(a,\omega)$

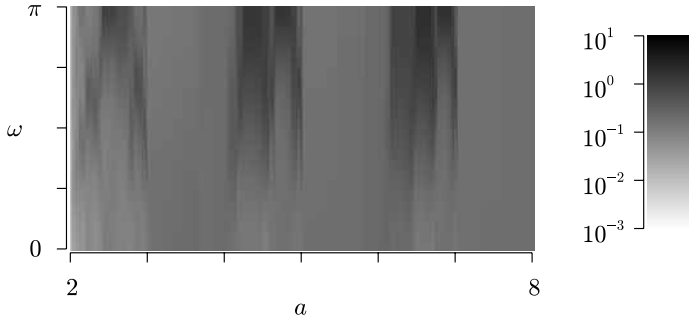

Figure 18: $I_{q=2}(a,\omega)$

Diffusion Fundamentals 3 (2005) 9.1 - 9.34

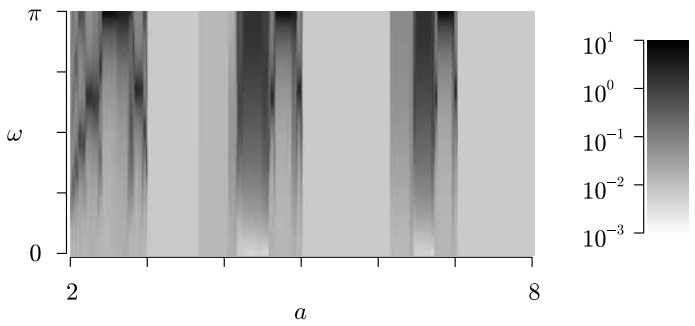

Figure 19: $I_{q=5}(a, \omega)$

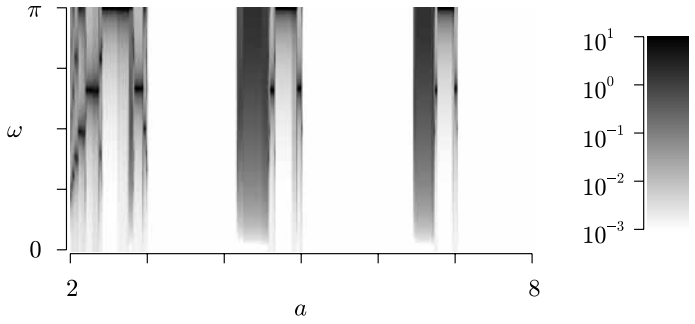

Figure 20: $I_{q=10}(a, \omega)$

Diffusion Fundamentals 3 (2005) 9.1 - 9.34

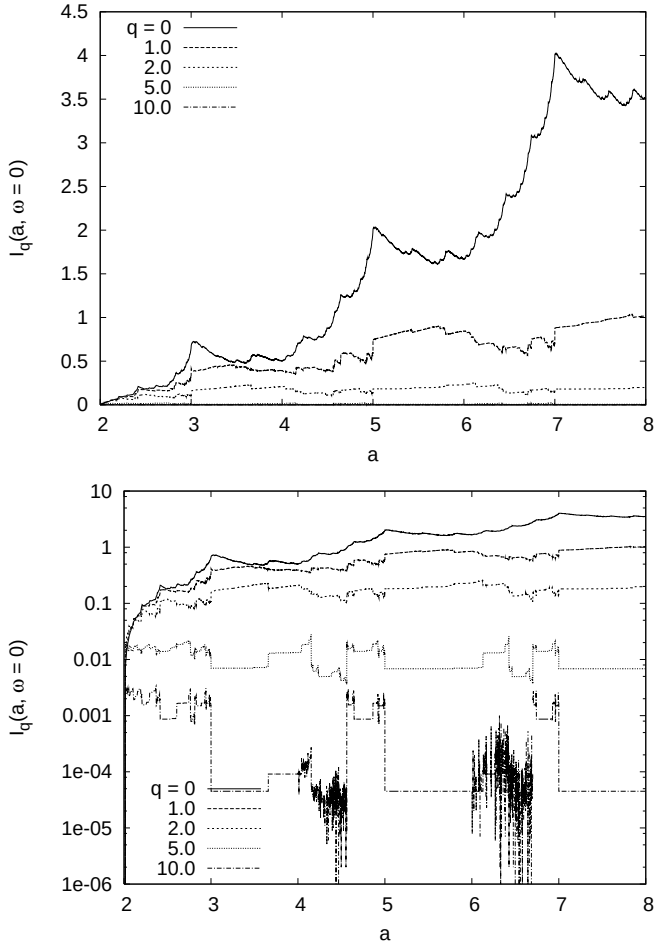

Figure 21: $I_q(a, \omega = 0)$

The lower graph in Fig. 21 contains some $q = 10$ parts which fluctuate markedly up and down. This seems to represent errors in calculation.

It is noticeable from these figures that the features of $I_q(a, \omega)$ differ greatly between the case of $q = 0$ and the case of larger q (particularly the case when $q = 10$). In Fig. 16, the plane $I_0(a, \omega)$ at $q = 0$ shows little change in the vertical direction, while it assumes higher values in the vertical direction as a increases. However, this increase is not a monotone increase but is really a repetition of small increases depending on the parameter as shown in the upper graph of Fig. 21 through 23. However, when $q = 10$ (Fig. 20), a region with relatively high values and a region with small values appear in an alternating manner in the horizontal direction. In

Diffusion Fundamentals 3 (2005) 9.1 - 9.34

the areas with large values in this case, the maximum value remains almost constant irrespective of an increase in a (see the lower graph in Fig. 21 through 23). Let us see the cell $2 \leq a \leq 3$ of the plane $I_q(a, \omega)$ when $q = 10$ (Fig. 20) in more detail. Figure 24 is a magnification of the cell $2 \leq a \leq 3$ of Fig. 20. In this cell, the plane $I_q(a, \omega)$ is a curve possessing one or multiple peaks in the locations satisfying $\omega = (l_a/m_a)\pi$ $(l_a, m_a \in \mathbb{Z}, l_a \leq m_a)$ when a is fixed at a certain value. In Sec. 3.3, we calculated the generalized power spectrum for $a = 1 + \sqrt{3}$ (a_1 in Fig. 24) in this area. Numerical calculation revealed that a sharp peak appears in the vicinity of $\omega = \pi$ when $q = 10$ (Fig. 10). In fact, when the a_1 in Fig. 24 is checked, the area in the vicinity of $\omega = \pi$ is black. When $q \to \infty$, this spectrum becomes a delta function which has values only at $\omega = \pi (= (1/2)2\pi)$, and the corresponding x_n time series was found to be period two drift orbits. The same can be said of a other than $a = a_1$. That is, the black gradational peak in the locations satisfying $\omega = (l_a/m_a)\pi = (l_a/2m_a)2\pi$ loses intermediate gray scales and becomes a black horizontal line when $q \to \infty$. As a result, the corresponding x_n motion may become a drift orbit with a period of $2m_a/l_a$. For example, in the cases of $a_2 = 2.1903\cdots$, $a_3 = 2.2207\cdots$ (Fig. 24), each spectrum has a peak at $\omega = \pi/3$, $\pi/4$ ($I_{q=10}(a_3, \omega)$ in Fig. 26 a has peak not only at $\pi/4$ but also at $\pi/2$.), and the weighted averages of the orbit's velocity $u(q)$ converge at $1/3$ and $1/4$, respectively, when $q \to \infty$ (Figs. 25-26). When $2 < a \leq 4$, it is evident that $\Delta(x'_n)$ assumed only three values $(0, 1, -1)$, in view of the shape of its map. Therefore, the time series of the drift orbit's velocity when $a = a_2, a_3$ and $q \to \infty$ will be defined as follows.

$$\{\Delta(x'_n)\} = \{\ldots, 0, 0, 1, 0, 0, 1, 0, 0, 1, 0, 0, 1, \ldots\} \, (a = a_2)$$

$$\{\Delta(x'_n)\} = \{\ldots, 0, 0, 0, 1, 0, 0, 0, 1, 0, 0, 0, 1, \ldots\} \, (a = a_3)$$

This area contains other spectra corresponding to drift orbits of varying periods of cycle, and the location of their peak is dependent on a in a complex manner. In Fig. 20, areas with a peak in the vertical direction are visible not only in the vicinity of $2 < a \leq 3$ but also in the vicinity of $4.55 \leq a \leq 5$ and $6.7 \leq a \leq 7$. These areas are the same in structure to the area $2 \leq a \leq 3$, except for the fact that they have been reduced in size in the horizontal direction.

4.3 Complex dependence of $u(q)$ on a

Some areas in Fig. 20 seem to be white, since the generalized power spectrum approaches a delta function located at the angular frequency corresponding to the period of the unstable periodic points causing the ballistic motion. For instance, in the seemingly white area in the vicinity of $a = 1 + \sqrt{3}$ the generalized power spectrum $I_q(\omega)$ is given by $\delta(\omega - \pi)$ in the limit of $q \to \infty$. The angular frequency $\omega = \pi$ corresponds to the period-2 unstable periodic points shown in Fig. 11, which also yield a ballistic motion shown in Fig. 12. In other seemingly white areas, $I_\infty(\omega)$ are found to be delta functions in the same way.

Diffusion Fundamentals 3 (2005) 9.1 - 9.34

To examine this in detail, let us see how the weighted average of the orbit's velocity $u(q)$ will converge when $q \to \infty$. Figure 27 graphically represents the relationship between parameter a and $u(q)$ when $q = 0$ to 10. Here, the partial differential related to q of $u(q)$ is $2D_q(a)$, according to Eq. (13). The curve of $D_q(a)$ (Fig. 14) shows that $D_{10}(a) \simeq 0$. We may therefore say that the graph of a, $u(10)$ at $q = 10$ (solid line in the graph) adequately converges to the graph of a, $u(\infty)$ at $q = \infty$. It seems therefore rational to deem the $q = 10$ graph as $q = \infty$. The $q = 10$ graph depicted with this solid line resembles the graph of a function called the "devil's staircase". Most of the graphs presenting the relationship between parameter a and the mean velocity of the drift orbit possessed by the corresponding mapping system (the mapping system with the highest velocity) have a gradient of 0 at most values of a. But their gradient shows a monotone increase as a increases when the entire graph is viewed.

In this graph, the value of $u(q \to \infty)$ when $3 < a < 4.2$ is 1. When $2 < a \leq 4$, the value of $\Delta(x'_n)$ are either 0, 1 or -1. Therefore at least in the range of $3 < a \leq 4$, the time series of the corresponding drift orbit's velocity assumes the following constant value.

$$\{\Delta(x'_n)\} = \{\ldots, 1, 1, 1, 1, 1, 1, 1, 1, 1, 1, 1, 1, \ldots\}$$

That is, since the frequency of the time series of the velocity is 0, the power spectrum of this time series, $I_\infty(a, \omega)$ has delta function values only when $\omega = 0$.

In the above-mentioned range $3 < a < 4.2$, an unstable fixed point is formed somewhere other than the point 0, 1 of the map g, and this point is 1 in the map Δ. Furthermore, in this range, the mean velocity of the fastest drift orbit, $u(q)$, assumes a value of 1. If the initial point is located immediately above this unstable fixed point under these conditions, the time series of $\Delta(x'_n)$ is 1 at all values of n. As a result, the power spectrum will become visible for the reasons mentioned above. The white appearance of the range $5 < a \leq 6.5$ can be explained by similar reasoning. In this case, the time series of $\Delta(x'_n)$ always assumes the value 2.

5 Conclusion

This paper dealt with extracting the non-Gaussian characteristics of the phenomenon of diffusion. The paper first referred to the fact that the diffusion coefficient can represent only Gaussian characteristics of diffusion, and discussed the generalization of the diffusion coefficient and power spectrum within the framework of the theory of large deviation statistics, with the goal of obtaining means for identifying both Gaussian and non-Gaussian characteristics. Then, the paper referred to the mapping system in which Klages and Dorfman discovered a complex dependence of diffusion coefficients on the parameter. We attempted to extract the non-Gaussian characteristics of this system by calculating the generalized diffusion coefficient D_q and the generalized power spectrum $I_q(\omega)$. The following results were obtained.

- The parameter of the system was set at $a = 1 + \sqrt{3}$, which is one of the

Diffusion Fundamentals 3 (2005) 9.1 - 9.34

simplest values allowing Markov partition. The statistical structure functions at that time, i.e., $\phi(q)$, $u(q)$ and $D_q(a)$, $I_q(a,\omega)$, were obtained analytically. When the velocity was set at the temporal coarse graining level, the motion corresponding to the physical process with largest deviation from the average was identified as the period two drift motion (Fig. 12).

- The curve representing the relationship between parameter a and $D_q(a)$ was numerically obtained for multiple q values (Fig. 14). This revealed that an increase in q leads to appearance of linear parts in the curve. We then attempted to evaluate the complexity of the curve quantitatively by obtaining the fractal dimension $d_f(q)$ for these $D_q(a)$ curves (Fig. 14).

- The two-dimensional field for a given value of q, i.e. $I_q(a,\omega)$, was numerically obtained (Figs.16-20). This disclosed that the motion corresponding to $q = \infty$ in this mapping system is a drift motion. It was also found that its period was dependent on parameter a in a complex manner.

- A graph plotting the weighted mean velocity $u(q)$ of diffusive particles against parameter a was numerically obtained (Fig. 27). This demonstrated that the graph $u(q \to \infty)$ corresponding to the average velocity of the drift orbit has a structure resembling the devil's staircase.

- It was found that the unstable periodic orbit of the map g corresponding to the drift motion with the highest velocity in this system changes in a complex manner depending on the value of parameter a. This seems to be one of the factors explaining why the graphs of $D_q(a)$ and $u(q)$ have complex structures.

The above-listed non-Gaussian characteristics of the chaotic diffusion system can be identified only within the framework of the theory of large deviation statistics. In this sense, we may say that the usefulness of the theory of large deviation statistics has been endorsed by this study.

The model used in this study is a model of diffusion applicable to quite limited conditions; it is a chaotic diffusion system created by piecewise linear mapping. Furthermore, the calculations made in this study used only the values of the parameter which allowed Markov partition of maps. Generally, it is not possible to analytically obtain the generalized Frobenius-Perron operator of maps in a given mapping diffusion system.

When performing calculation of the variables like the ones listed above related to deterministic diffusion (occurring from maps) as well as general diffusion, it is necessary to numerically obtain statistical structure functions from the temporal coarse graining levels of the observed variables, and to deduce from these the generalized diffusion coefficient D_q and the generalized power spectrum $I_q(\omega)$. It will be difficult to plot complex parameter dependences of generalized diffusion coefficients obtained numerically. Takagi function-like behaviors might hide behind numerical errors. In contrast, devil's staircase like parameter dependences of a ballistic velocity $u(\infty)$ will be relatively easily obtained for general deterministic diffusive

Diffusion Fundamentals 3 (2005) 9.1 - 9.34

systems. We have only to numerically find the most deviated coarse-grained velocity from the average, which is related to a single unstable periodic trajectory.

One of the open issues related to chaotic diffusion by piecewise linear mapping is to make similar calculations for maps different from those used in this study, and to examine whether or not the dependency on the parameter of the maps and other features revealed in this study are commonly seen in other piecewise linear mapping systems. Another open issue is to numerically obtain statistical structure functions, generalized diffusion coefficients, etc., not only in models of mapping systems but also in actual experimental systems, with the goal of examining how the non-Gaussian characteristics will be reflected in the results.

Acknowledgements

This study was partially supported by the 21st Century COE Program "Center of Excellence for Research and Education on Complex Functional Mechanical Systems "at Kyoto University.

A Methods for calculation of parameter a which allows Markov partition

If the time series $\{x_n\}$ satisfies a certain requirement, $\{x_n\}$ can divide unit interval into only a finite number of intervals. The requirement is that the time series $\{x_n\}$ becomes a periodic orbit after the time n^* $(0 \leq n^* < \infty)$. (This contains the case that $\{x_n\}$ falls on a fixed point at time n^*.) If this requirement is satisfied, map g can be subjected to Markov partition, with these cells serving as Markov cells. That is, if a value of parameter a satisfying this requirement can be identified, it is possible to obtain the matrix $H_q(a)$ of the generalized Frobenius-Perron operator for the map g, corresponding to that value of a, and to calculate statistical structure functions $D_q(a)$ and $I_q(a,\omega)$ from the maximum eigenvalue $\nu_q^{(0)}(a)$ of $H_q(a)$.

When identifying these values of a in a comprehensive manner, using a computer, it is advisable to use the following method. The piecewise linear mapping (23) involves arrangement of maps composed of segments with gradient a and length $\sqrt{1+a^2}$. For reasons of convenience, these maps are named $f_N(N \in \mathbb{N})$ as shown in Fig. 28. These segments can then be expressed as follows:

$$y = f_N(x) \equiv a(x-N)+N, \ \left(N - \frac{1}{2} < x \leq N + \frac{1}{2}\right).$$

If the points at the upper edge, lower edge and center of the segment defined by $y = f_N(x)$ are denoted as A_N, B_N and C_N, we may say as follows:

"If the parameter a of the entire map f is set at a certain value and the point after i times of mapping of the initial point $1/2$ is consistent with one of A_N, B_N

Diffusion Fundamentals 3 (2005) 9.1 - 9.34

and C_N ($N \in \mathbb{N}$), the map f can be subjected to Markov partition at that value of parameter a."

In this case, the map g, obtained by deformation of the map f, can also be subjected to Markov partition. What should be done is therefore to identify a value of a which satisfies this condition, using a computer.

Let us consider a case where the value of a, which allows the initial point to be mapped to $A_2 = (2+1/2, f_2(2+1/2)$ through 3 rounds of mapping, is to be obtained. The orbit between the initial point and A_2 can be expressed as follows. There are an infinite number of pathways between them, instead of only one pathway, as shown below.

$$\begin{aligned}
&\frac{1}{2} \xrightarrow{f_0} x_1 \xrightarrow{f_1} x_2 \xrightarrow{f_2} 2 + \frac{1}{2}, \\
&\frac{1}{2} \xrightarrow{f_0} x_1 \xrightarrow{f_1} x_2 \xrightarrow{f_1} 2 + \frac{1}{2}, \\
&\frac{1}{2} \xrightarrow{f_0} x_1 \xrightarrow{f_2} x_2 \xrightarrow{f_1} 2 + \frac{1}{2}, \\
&\vdots
\end{aligned}$$

What is required is therefore to list these possible pathways using a computer and to prepare algebraic equations for each pathway, in order to obtain a solution through numerical calculation. Although the equation corresponding to these pathways can be prepared in an infinite number, this prepared equation does not always have a solution expressed in a real number. Furthermore, since a is limited to $a > 2$, only a small number of equations will yield a solution.

References

[1] T. Geisel and J. Nierwetberg, Phys. Rev. Lett. **48**, 7 (1984).

[2] H. Fujisaka and M. Inoue, J. Phys. Soc. Jpn. **70**, 2283 (2001).

[3] R. Klages and J. R. Dorfman, Phys. Rev. Lett. **74**, 387 (1995).

[4] H. Fujisaka and M. Inoue, Prog. Theor. Phys. **77**, 1334 (1987).

[5] H. Fujisaka and M. Inoue, Phys. Rev. A **41**, 5302 (1990).

[6] H. Fujisaka and H. Shibata, Prog. Theor. Phys. **85**, 187 (1991).

[7] M. Inoue and H. Fujisaka, Phys. Rev. B **32**, 277 (1985).

[8] T. Kobayashi, H. Fujisaka, and W. Just, Phys. Rev. E **47**, 3196 (1993).

[9] W. Just and H. Fujisaka, Physica D **64**, 98 (1993).

Diffusion Fundamentals 3 (2005) 9.1 - 9.34

[10] H. G. Schuster, *Deterministic Chaos*, third augmented edition, VCH, Weinheim (1995).

[11] S. Grossmann and H. Fujisaka, Phys. Rev. A **26**, 1779 (1982).

[12] H. Fujisaka and S. Grossmann, Z. Phys. B **48**, 261 (1982).

[13] R. Klages, *Deterministic Diffusion in One-Dimensional Chaotic Dynamical Systems*, Wissenschaft und Technik Verlag, Berlin (1996).

[14] R. Klages and J. R. Dorfman, Phys. Rev. E **59**, 5361 (1999).

[15] R. Klages, Phys. Rev. E **65**, 055203(R) (2002).

Diffusion Fundamentals 3 (2005) 9.1 - 9.34

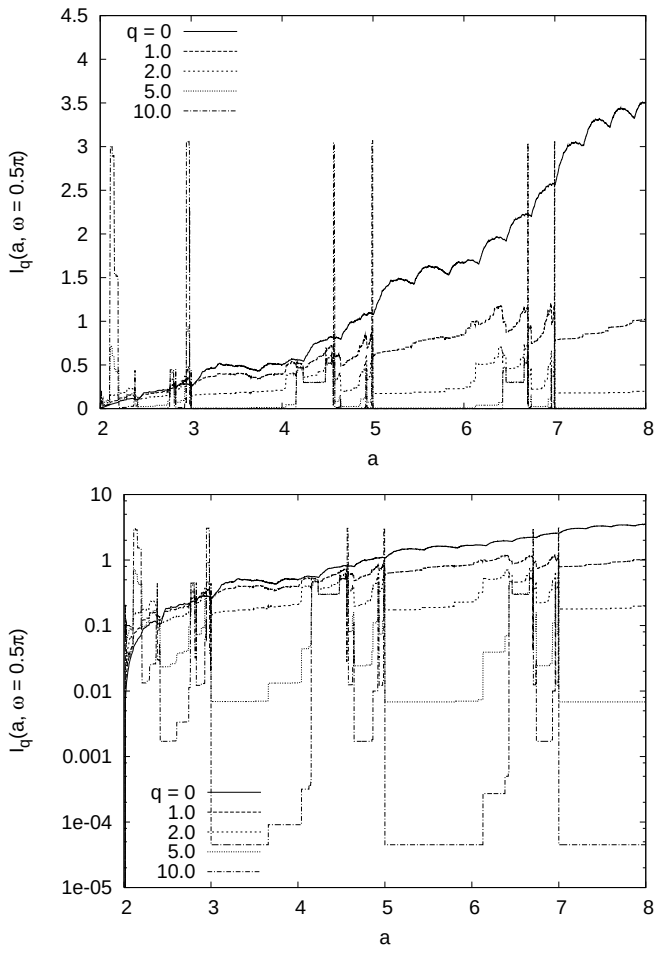

Figure 22: $I_q(a, \omega = \frac{1}{2}\pi)$

Diffusion Fundamentals 3 (2005) 9.1 - 9.34

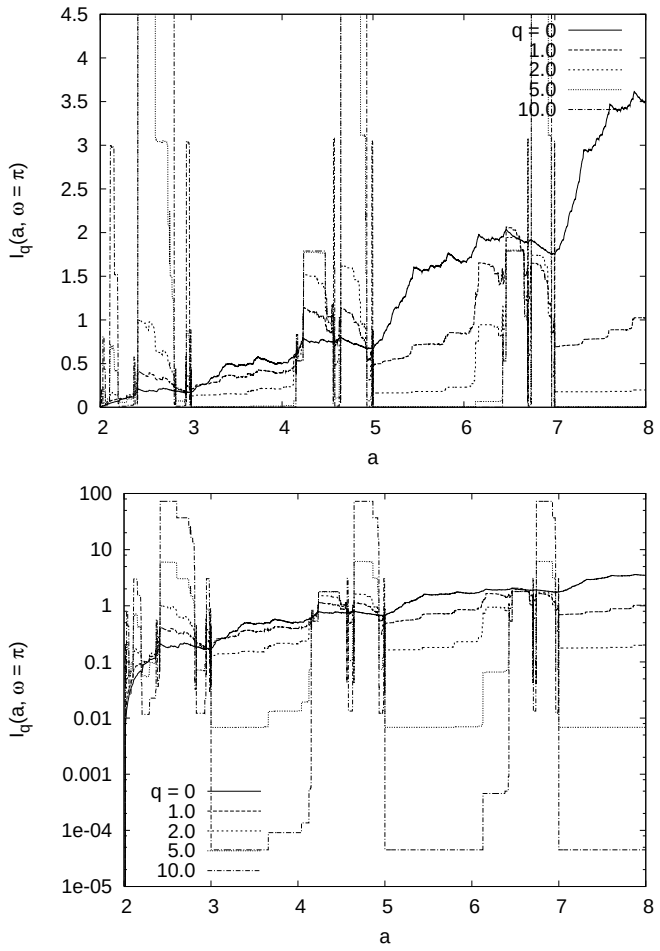

Figure 23: $I_q(a, \omega = \pi)$

Diffusion Fundamentals 3 (2005) 9.1 - 9.34

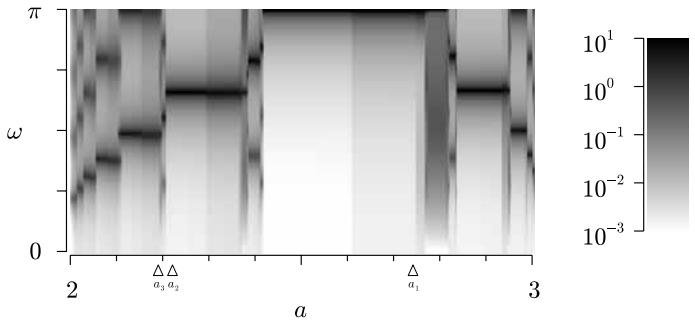

Figure 24: $I_{q=10}(a, \omega)$ for $2 \leq a \leq 3$

Diffusion Fundamentals 3 (2005) 9.1 - 9.34

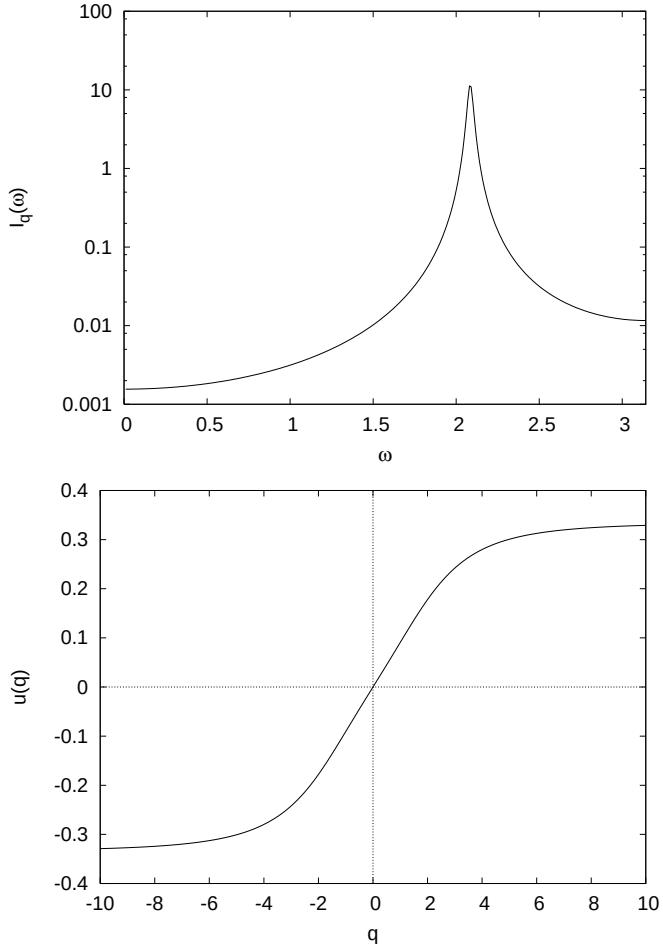

Figure 25: $I_{q=10}(a_2, \omega)$ and $u(q)$ at $a = a_2 (= 2.1903\ldots)$

Diffusion Fundamentals 3 (2005) 9.1 - 9.34

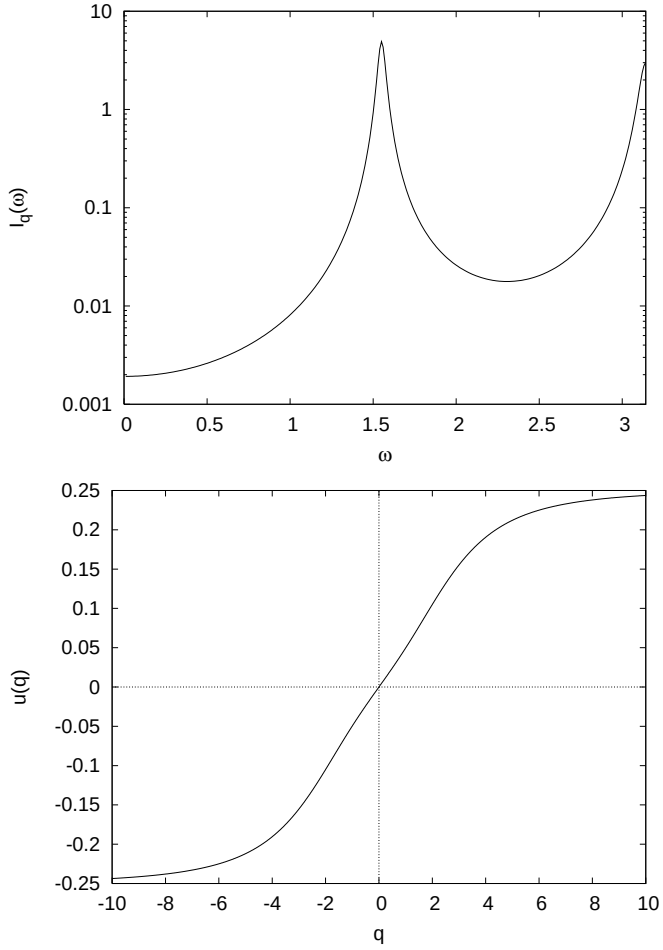

Figure 26: $I_{q=10}(a_3, \omega)$ and $u(q)$ at $a = a_3 (= 2.207\ldots)$

Diffusion Fundamentals 3 (2005) 9.1 - 9.34

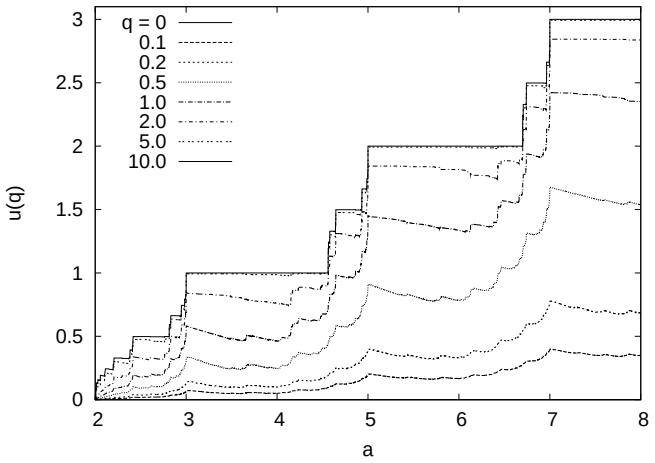

Figure 27: Relation between a and $u(q)$

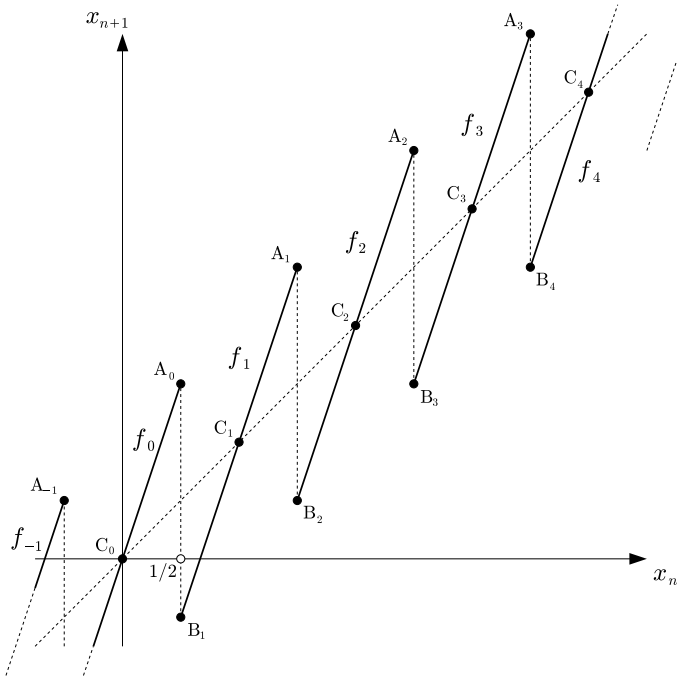

Figure 28: Points $\mathrm{A}_N, \mathrm{B}_N, \mathrm{C}_N$ on the map f_N

Diffusion Fundamentals 3 (2005) 9.1 - 9.34